Sea-floor and sea-ice conditions in the western Weddell Sea, Antarctica, around the wreck of Sir Ernest Shackleton's *Endurance*

J.A. Dowdeswell [a], C.L. Batchelor [a,b], B. Dorschel [c], T.J. Benham [a], F.D.W. Christie [a], E.K. Dowdeswell [a], A. Montelli [a], J.E. Arndt [c], C. Gebhardt [c]

[a] *Scott Polar Research Institute, University of Cambridge, Cambridge CB2 1ER, UK*
[b] *Norwegian University of Science and Technology (NTNU), NO-7491, Trondheim, Norway*
[c] *Alfred Wegener Institute, Helmholtz Centre for Polar and Marine Research, Bremerhaven, Germany*

Abstract: Marine-geophysical evidence on sea-floor morphology and shallow acoustic stratigraphy is used to examine the substrate around the location at which Sir Ernest Shackleton's ship *Endurance* sank in 1915 and on the continental slope-shelf sedimentary system above this site in the western Weddell Sea. Few signs of turbidity-current and mass-wasting activity are found near or upslope of the wreck site, and any such activity was probably linked to full-glacial higher-energy conditions when ice last advanced across the continental shelf. The wreck is well below the maximum depth of iceberg keels and will not have been damaged by ice-keel ploughing. The wreck has probably been draped by only a few centimetres of fine-grained sediment since it sank in 1915. Severe modern sea-ice conditions hamper access to the wreck site. Accessing and investigating the wreck of *Endurance* in the Weddell Sea therefore represents a significant challenge. An ice-breaking research vessel is required and even this would not guarantee that the site could be reached. Heavy sea-ice cover at the wreck site, similar to that encountered by *Agulhus II* during the Weddell Sea Expedition 2019, would also make the launch and recovery of AUVs and ROVs deployed to investigate the *Endurance* wreck problematic.

Key words: acoustic stratigraphy, continental shelf, continental slope, icebergs, seafloor landforms

Introduction

Sir Ernest Shackleton's ship *Endurance* was trapped in the drifting sea ice of the Weddell Sea, Antarctica, for over 10 months before finally sinking on 21 November 1915 (Fig. 1). Prior to being beset in the ice, the ship had intended to land Shackleton and his 27-man party on the East Antarctic coast to attempt the first crossing of the continent on what was known as the 'Imperial Trans-Antarctic Expedition' (Shackleton, 1919). After the sinking of *Endurance* there followed a prolonged encampment on the drifting sea ice, a journey in three small open-boats to Elephant Island, where the main group of 22 men remained, and then an epic 1,300 km voyage across the Southern Ocean to South Georgia by Shackleton and five companions in the 6.6 m-long '*James Caird*' to raise the alarm and organise a rescue (Fig. 1) (Shackleton, 1919; Worsley, 1931).

The site at which Shackleton's *Endurance* sank is in about 3,000 m of water on the lower continental slope about 300 km east of Larsen C Ice Shelf, the terminus of which forms the longest coastal ice cliffs on the eastern side of the Antarctic Peninsula (Fig. 1). The location is relatively well-known, although some uncertainties remain. Bergman and Stuart (2018) re-analysed the original theodolite- and sextant-derived astronomical observations made at the time the ship sank by Captain Frank Worsley of the *Endurance*. Worsley's astronomical observations, now held in an historic archive at the Canterbury Museum, Christchurch, New Zealand, suggest that the ship sank at 68°39'30"S 52°26'30"W. These observations have been re-analysed subsequently to produce a small 'search box' within which the vessel is likely to lie on the sea-floor (Bergman and Stuart, 2018).

The main aim of this paper is to consider the nature of the sea-floor in the vicinity of the wreck site, together with the geological processes operating today on the continental margin (slope and shelf) upslope of the wreck site, westwards towards the Antarctic Peninsula; these include the possible action of erosive and depositional processes that might impede finding the wreck. Despite the fact that the western Weddell Sea is an area of almost complete sea-ice cover in most years, even during the austral summer, limited marine-geophysical data in the form of multibeam echo-sounding and shallow sub-bottom profiling have been acquired from icebreaking research vessels. These data are used to investigate the morphology and geological processes on the shelf and slope adjacent to the wreck site. Additionally, we characterise the sea-ice cover typically found in the western Weddell Sea, which makes access to the wreck site difficult in most years and almost impossible in some, even for vessels with significant icebreaking capability.

Methods

The multibeam swath-bathymetric observations and shallow sub-bottom profiler data used in this paper were collected by the Alfred Wegener Institute's (AWI) icebreaking Research Vessel (RV) *Polarstern* on several scientific cruises in the Weddell Sea between 1993 and 2011: ANT X/7 (1993; Bathmann et al., 1994; Schenke, 2011), ANT XIV/3 3 (1997; Dijkstra et al., 2011; Jokat & Oerter, 1998), ANT XIX/2 (2001/02; Jokat & Gunther, 2003; Schenke et al., 2004), ANT XXII/2 (2004/05; Beyer et al., 2007; El Naggar et al., 2007; Schenke et al., 2009), ANT XXIII/8 (2006/07; Gutt, 2008; Gutt et al., 2010), ANT XXVII/3 (2011; Fillinger et al., 2011), available at doi.org/10.1594/PANGAEA. Severe sea-ice conditions made navigation difficult and sometimes reduced data quality. The frequent changes of course on the ship tracks close to the *Endurance* wreck site are examples of the ship navigating through heavy sea ice (Figs. 2a, 3, 4a), a situation all too familiar to that of Sir Ernest Shackleton and his party almost one hundred years earlier (Figs. 1b and 2a).

The multibeam equipment used for bathymetric data acquisition from RV *Polarstern* was hull-mounted 2°×2° Hydrosweep DS1 (01.08.1989 – 01.10.1997), DS2 (10.10.1997 – 10.10.2010) or DS3 (since 20.10.2010) multibeam systems manufactured by Atlas Hydrographic. The systems operated in a range of frequencies of 13-17 kHz with 59 beams (DS1, DS2), and 141 beams (DS3) and a beam-aperture of up to 120°. The raw data were processed using CARIS HIPS and SIPS® and QPS Fledermaus® software and gridded at a cell-size of 100 m.

Sub-bottom profiler data were acquired using a hull-mounted Atlas PS70 PARASOUND system, manufactured by Atlas Hydrographic, applying a mean water sound-velocity of 1,500 m s^{-1}. Heavy sea ice caused noisy returns with missing traces on some occasions. The system used the parametric effect and sends out energy at two primary frequencies (normally 18 and 22 kHz) that produce a secondary pulse at a lower frequency (usually 4 kHz). Vertical resolution is 30 cm or better. Penetration depth of the sub-bottom profiler can reach several tens of metres in fine-grained and well-sorted sediments, but is reduced considerably in diamictic material. In this paper, the PARASOUND data were classified visually into four acoustic facies (e.g. Damuth, 1978; Dowdeswell et al., 2010); Facies A – acoustically impenetrable sea-floor; Facies B – highly irregular sea-floor; Facies C – lenses; Facies D – acoustically stratified (Fig. 4).

Satellite data concerning sea-ice cover over the Weddell Sea were derived from a combination of daily NASA Worldview multispectral (visible, NIR and SWIR; 256 m

resolution) and thermal band (1024 m resolution) mosaics of: Moderate Resolution Imaging Spectroradiometer (MODIS) imagery from the Terra (EOS AM-1) and Aqua (EOS PM-1) satellites; and Visible Infrared Imaging Radiometer Suite (VIIRS) imagery from Suomi NPP satellite. These datasets were employed due to their higher spatial resolution relative to conventional passive-microwave based observations (e.g. Zwally & Gloersen, 1977; Comiso et al., 2008; Vernet et al., 2019), allowing for more detailed depiction of the sea-ice cover. Data were acquired free of charge in GeoTIFF format from the Global Imagery Browse Services (GIBS; earthdata.nasa.gov/gibs) web facility, which underpins the NASA EOSDIS Worldview data portal (https://worldview.earthdata.nasa.gov). These datasets were then processed to form daily composites of (as far as possible) cloud-free image coverage, in order to classify sea-ice and open-water occurrence, and to estimate the ice concentration in 'sea ice'-classified pixels (with reference to image-specific statistics from 'water' and 'sea ice' initial classifications). From these daily concentration maps, we then summarized the average summertime sea-ice cover (December, January, February) of the western Weddell Sea, including the *Endurance* wreck site, for the period covered by the source imagery, from 2002 to present.

The location where *Endurance* sank clearly defines the downslope end of our study area. There are, however, some relatively small uncertainties in this position due to factors including: the fact that Captain Worsley made no astronomical observations between three days before and nearly 16 hours after the sinking; the drift of the chronometer used (primarily affecting longitude); the exact distance and bearing between 'Ocean Camp' and the *Endurance*; and the speed and bearing of sea-ice drift assumed for dead reckoning of position. Bergman and Stuart (2018) suggested a latitudinal limit of 4.5 nautical miles to bound the sinking location, and we interpret their findings regarding longitude accuracy to yield an approximately 13 NM range in the east – west axis. Further uncertainty is added by lack of knowledge of exact offsets between positions recorded in 1915 and the modern-day WGS84 datum (albeit likely to be within ~400 m), and of any horizontal displacement between the point of sinking and the wreck's sea-floor location. In the latter case, the drag caused by remaining vessel masts and yards suggests that the vessel's path to the sea floor would not have differed greatly from the vertical.

Marine-geophysical observations of the sea-floor

At present, only a limited amount of multibeam swath-bathymetric data are available for the approximately 400,000 km^2 area illustrated in Figure 2a. The area comprises the shelf-

slope system present eastward of the ice cliffs of Larsen C Ice Shelf, extending across the almost 200 km-wide continental shelf and descending to over 3,500 m deep beyond the wreck site of *Endurance*. The multibeam data coverage of the study area is shown in Figure 2a, and the accompanying regional bathymetry is from the International Bathymetric Chart of the Southern Ocean (IBCSO; Arndt et al., 2013). The IBCSO data are gridded at a cell-size of 500 m and are interpolated between actual observations of water depth, which, in the study area, are comprised almost exclusively of the multibeam echo-sounder data collected by RV *Polarstern* and shown here in detail.

Continental shelf offshore of Larsen C

Evidence from multibeam echo-sounding shows that much of the sea-floor offshore of Larsen C Ice Shelf is incised by irregular, linear to curvilinear depressions (Figs. 2a, 3b). The depressions are present in water depths of between 280 and 620 m (Fig. 3a), and are up to 200 m wide and 10 m deep (Fig. 3a, b). These features are interpreted as iceberg ploughmarks that are formed by the grounding of iceberg keels in sea-floor sediments (e.g. Dowdeswell and Bamber, 2007). The depth of most of the iceberg ploughmarks in the western Weddell Sea is significantly greater than the deepest draft of modern Larsen C-derived icebergs (Fig. 3a; Dowdeswell and Bamber, 2007), suggesting that most of the ploughmarks were produced during the last deglaciation. There are no dated cores on the continental shelf offshore of Larsen C Ice Shelf; however, cores from the mouth of Prince Gustav Channel near the north-eastern tip of the Antarctic Peninsula suggest that deglaciation probably took place between about 13.6 and 10.7 kyr ago (Evans et al., 2005; Pudsey et al., 2006; Ó Cofaigh et al., 2014). Thus, the continental shelf beyond Larsen C Ice Shelf is likely to have been free of ice for at least the last 10,000 years.

The shallow acoustic stratigraphy of the continental shelf beyond Larsen C Ice Shelf is characterised mainly by Facies B, which comprises a 5-20 ms-thick (*c*.5-20 m) semi-transparent unit underlying a highly irregular sea-floor (Fig. 4a, c). This acoustic facies corresponds with the distribution of iceberg ploughmarks on the bathymetric data (Figs. 2a and 4a) and is interpreted as sediment that has been reworked by the keels of grounding icebergs (also referred to in the literature as "iceberg turbate") (e.g. Hillenbrand et al., 2005; Campo et al., 2017).

Continental slope of the western Weddell Sea

Most of the continental slope of the western Weddell Sea is relatively featureless at the 100 m grid-cell size of our bathymetric data (e.g. Fig. 2b). However, there is some evidence for slope disturbances in the form of abrupt changes in slope gradient and submarine channels (Fig. 3c, d), particularly beyond Robertson and Jason troughs to the north of the study area (Fig. 2a). A slide scar, with a headwall up to 60 m high and a sea-floor gradient of around 20°, is present on the upper slope beyond the southern edge of Robertson Trough (Figs. 2a, 3c). About 50 km further downslope of the slide scar, IBCSO bathymetry data suggest that a series of gullies extends between around 1,200 and 3,000 m water depth (Fig. 2a). These features imply that this area has been affected by slope failures.

Several low sinuosity submarine channels, up to 1 km wide and 50 m deep, are present on the middle to lower continental slope (Figs. 2a, 3d). Individual channels can be traced for up to 100 km, although they most likely extend for significant lengths beyond the limit of our bathymetric data (Fig. 2a). The channels were probably formed by turbidity currents that were triggered by the delivery of turbid meltwater from ice sheets, dense-water formation through brine rejection during sea-ice formation, debris flows and/or other mass movements (e.g. Dowdeswell et al., 2008).

In terms of distribution of acoustic facies, the continental slope can be divided into three broad areas (Fig. 4a). Facies A (Fig. 4b) is generally present on the upper slope, where the lack of acoustic penetration suggests that the sea-floor contains relatively hard sediment that is probably diamictic (e.g. Anderson, 1999). Facies C, which comprises stacked acoustically transparent lenses up to 30 ms (30 m) thick, is present on the mid-slope between 1,000 and 3,400 m water depth (Figs. 4a, d and 5). The geometry and dimensions of the lenses suggests that they are glacigenic debris-flows (GDFs) that were produced by the remobilisation of deformable diamictic sediments that were delivered to the shelf break and upper slope by the Antarctic Peninsula Ice Sheet during full-glacial conditions about 20,000 years ago (King et al., 1998; Hillenbrand et al., 2005). The lenses are draped by an acoustically stratified unit that is up to 10 ms (10 m) thick (Figs. 4d, 5b, c), which was probably formed by the deposition of hemipelagic debris in a relatively low-energy environment.

In water depths greater than around 2,400 m, the lower continental slope is characterised by Facies D, which has a stratified acoustic character and an acoustic penetration depth of up to 50 ms (50 m) (Fig. 4a and e). This is again likely linked to the slow rain-out of hemipelagic debris. The lower slope, therefore, probably contains relatively fine-grained and well-sorted sediment that was deposited in a low-energy, ice-sheet-distal environment.

Wreck site

In the area of the *Endurance* wreck the sea-floor appears almost flat in the swath-bathymetric data (Fig. 2b), with a slope angle of no more than 0.3° (Fig. 5) and a water depth of about 3,000 m. In contrast to other regions of the continental margin, no sea-floor disturbances, including iceberg ploughmarks, sediment slides, channels or gullies (e.g. Fig. 3), are apparent in the vicinity of the wreck site (Fig. 2). The multibeam data on the sea-floor collected by RV *Polarstern*, which cover part of the wreck-site search box (Fig. 2a), do not appear to show any evidence of the 44 m-long and 7.6 m-wide wreck (Fig. 2b), although the 100 m grid-cell size of the data should be remembered, as well as the 'noisiness' of the data due to navigation through sea ice. Most of the structure apparent in the bathymetric dataset is probably artefactual and includes the effects of the ship turning close to Worsley's reckoning of the location of the expedition's 'Ocean Camp' (Fig. 2b). There are also multibeam signal dropouts near the edges of the mosaic and several subtle sub-linear features; the latter are again artefacts probably related to the switching of multibeam bottom-detection algorithms between the use of phase and amplitude data collected relatively close to the nadir point beneath the vessel (Jakobsson et al., 2016).

Sub-bottom profiler data from the same area show acoustic penetration to about 20-30 ms (approximately 20-30 m) below the sea-floor (Fig. 5a and c). There is evidence of acoustic lamination together with the pinching out of a lens of debris in the downslope direction (Fig. 5c). The area of the search box therefore appears to contain some characteristics of acoustic Facies C and D (Fig. 4). Persistent acoustically laminated material would suggest slow deposition of hemipelagic debris in a low-energy environment, and this appears to characterise at least the uppermost 10 ms (10 m) of the record (Fig. 5c). Beneath this, there is evidence of the pinching out of a sediment lens, which implies downslope mass wasting, with the profile in Figure 5c imaging the distal toe of such an event. However, given that the upper part of this lens is buried by around 10 m of sediment, it is likely that low-energy conditions have persisted for some time in the vicinity of the *Endurance* wreck and that slow sedimentation of hemipelagic debris has characterised sedimentation here over the past century. Indeed, typical deep-water sedimentation rates in dated sediment cores from the similar deep-water settings in the Weddell Sea suggest rates of less than a millimetre per year (Anderson and Andrews, 1999), implying that the uppermost 10 m of crudely laminated sediments in the sub-bottom profile closest to 'Ocean Camp' shown in Figure 5c probably represents a multi-millennial period of low-energy conditions. This implies, in turn, that the wreck of Shackleton's *Endurance* is unlikely to have been disturbed by recent submarine

mass-wasting events and that it is being buried only very slowly by modern sedimentation. With cut-down masts and yards trailing behind, drag would have been imposed on the sinking hull, likely reducing the seabed impact velocity of *Endurance*. We therefore assume that *Endurance* settled on the seabed keel-first, without significant penetration of sea-floor sediments.

Surface sea-ice conditions

Satellite observations

Sea ice persists through the austral summer in the Weddell Sea, especially on its western side including in front of Larsen C Ice Shelf (Fig. 6a). The sea-ice extent generally reaches a minimum in February, with the sea-ice edge typically spanning from west of Brunt Ice Shelf in the eastern Weddell Sea to James Ross Island off the eastern Antarctic Peninsula (Fig. 1a). As sea ice does not generally re-enter the Weddell Gyre to the east, the age of most of the sea ice in the western Weddell Sea is probably less than about two years (Kottmeier et al., 1997). Estimates of the mean thickness of unridged sea ice from satellite laser altimetry range between 0.4 and 2 m across this region (Kurtz and Markus, 2012), although maximum ice thicknesses may significantly exceed this value, for example due to pressure ridges (Tan et al., 2012). Since the decommissioning of the ICESat GLAS laser altimeter in 2009, no routine sea-ice thickness products are available, prohibiting inter-annual comparison of regional thicknesses and ridging across the Weddell Sea. The distribution and concentration of sea ice in the western Weddell Sea (Fig. 6a) clearly presents a significant challenge to any expedition that seeks to access the wreck site of the *Endurance*.

Our maps of average December-January-February sea-ice concentration in the western Weddell Sea between 2002 and 2019, produced from MODIS and VIIRS optical and thermal imagery, were assessed qualitatively by six independent scientists as 'Good', 'Intermediate' or 'Bad' in terms of overall sea-ice navigability (Fig. 6e). Examples of 'Good', 'Intermediate' and 'Bad' sea-ice conditions are shown in Figure 6b-d, respectively. These qualitative rankings are based on: (i) the proximity of the *Endurance* wreck site to open water; and (ii) sea-ice concentration at the *Endurance* wreck site. We also took into account ancillary information, including reference sea-ice thickness (Worby et al., 2008; Kurtz & Markus, 2012), as well as knowledge of the actual conditions experienced in the area by the Weddell Sea Expedition in February 2019 versus our average concentration map for that month (ship-tracks shown in Figure 6c). Note that we refer to individual austral summer periods below

according to the year of the January and February of that season: e.g. December 2003 to February 2004 is referred to as '2004'.

For the last 18 years, average December-January-February sea-ice conditions in the western Weddell Sea have been, in our assessment, generally 'Intermediate' or 'Bad' (Fig. 6e) for access to the *Endurance* wreck site. An exception was in 2002, when significant regions of low sea-ice concentration were present in the central western Weddell Sea (Fig. 6b), enabling the Alfred Wegener Institute's research icebreaker RV *Polarstern* to navigate close to the estimated wreck location (Fig. 2). Since 2002, three (17%) of the years are categorised as showing 'Intermediate' sea-ice conditions, in which the wreck search area was generally <200 km from open water and in 90-100% sea ice concentration (Fig. 6c and e). However, 14 (78%) of the assessed years show 'Bad' sea-ice conditions, in which the wreck search area was generally >200 km from open water and in 100% sea-ice concentration (Fig. 6d and e). In early February 2019, the South African research vessel SA *Agulhas II* navigated to the wreck search area as part of the Weddell Sea Expedition 2019 (Fig. 6c). Although an autonomous underwater vehicle (AUV) was successfully deployed within the wreck search area, SA *Agulhas II* lost contact with the AUV and worsening sea-ice conditions meant that the search had to be abandoned with no AUV multibeam data retrieved.

No clear trend of decreasing or increasing sea-ice concentration in the western Weddell Sea has been identified over the observational period, although sea-ice conditions in the last 10 years have been generally poor (Fig. 6e). Notable inter-annual differences in summertime sea-ice cover are observed; for example, inter-annual fluctuations between upper 'Intermediate' and 'Bad' sea ice conditions occurred between summers 2009 and 2010 (Fig. 6e). For the past 18 years, the most favourable patterns of sea-ice concentration for wreck-site access have generally occurred in February (Fig. 6e). Notable exceptions are in summers 2007, 2009 and 2012, when we assessed the most favourable conditions to have occurred in January, and in summer 2011, when the easiest access was in December (2010). Assessments of sea-ice navigability in the western Weddell Sea are complicated by the highly changeable nature of the sea-ice conditions, whereby areas of open water, including near-shore leads, can open and close within a timescale of a few days. Our findings are consistent with contemporaneous but lower resolution passive-microwave derived sea-ice concentration products (Cavalieri et al., 1996). In addition, examination of passive microwave data on Weddell Sea sea-ice conditions from 1978 to 2002 suggests just a few years similar to our observations from 2002; the austral summers of 1981, 1987, 1993 and 1999 were each relatively good years for navigation in the western Weddell Sea.

Major iceberg calving events can also affect sea-ice distribution and concentration, further complicating predictability of ice conditions. As an example, the calving from Larsen C Ice Shelf in July 2017, and subsequent grounding of iceberg A-68 between June and November 2018 (Fig. 6a), may have impeded the northerly flow of sea ice in the western Weddell Sea, which typically drifts in a clockwise direction associated with the cyclonic Weddell Gyre (e.g. Deacon, 1979; Muench and Gordon, 1995). The barrier-like effect of icebergs such as A-68 are therefore presumably analogous to the protective effects of ice tongues on local sea-ice concentration across other parts of Antarctica (e.g. Miles et al., 2017).

The Weddell Sea Expedition 2019

In early February 2019, the South African research vessel SA *Agulhas II* navigated to the wreck search area as part of the Weddell Sea Expedition 2019. Transit to the wreck site was facilitated by a progressive opening in the eastern edge of the sea-ice margin, which extended to within 170 km of the wreck site (Figs. 6c, 7a) – a phenomenon not observed on MODIS imagery throughout most of its observational record. Approaching the wreck site from this direction, an associated loosening of the pack ice resulted in the presence of several large leads (Fig. 7a) that the vessel was able to exploit despite the still heavy (~90%+) sea-ice concentration. Sea-ice thicknesses ranging from ~2 to 5 m (mean ~ 2.5 m) were observed during this approach to and within the search area. These values exceed the thickness data provided by earlier ship observations (Worby et al., 2008), and fall within the upper limits of estimates derived from satellite laser-altimetry (Kurtz & Markus, 2012; Kern et al., 2016). These thickness values were also in good agreement with synoptic sea-ice thickness forecasts from the Copernicus Marine Environment Monitoring Service (CMEMS) Global Ocean 1/12° physics analysis and forecast model (Lelouche et al., 2019). Within the wreck search area occasional patches of rotten ice were also encountered, and were composed of honeycombed multi-year ice probably conditioned by summertime surface melting events (Frantz et al., 2019).

The presence of open-water sea-ice leads, at times extending to greater than 900 m and 700 m in length and breadth, respectively, persisted well within the search box (Fig. 7b-c). These leads allowed the successful deployment of a Hugin-6000 autonomous underwater vehicle (AUV) tasked with locating and surveying *Endurance*. Unfortunately, SA *Agulhas II* later lost communication with the AUV after initially tracking it on several survey lines close to the seafloor. Worsening sea-ice conditions meant that the search for the AUV had to be

abandoned with no multibeam data retrieved. The reasons for the loss of the AUV remain unknown.

Discussion

Marine-geophysical evidence in the form of multibeam swath-bathymetry and acoustic sub-bottom profiling shows that sea-floor in the proximity of the wreck of Shackleton's *Endurance* is of very low gradient and likely to be composed of fine-grained hemipelagic sediment (Fig. 5). The very slow rates of sedimentation in the deep waters of the Weddell Sea also suggest that the wreck itself is unlikely to have been draped by more than a few centimetres of silt and clay in the century since it sank.

In addition, the relatively smooth morphology and acoustic character of the sea-floor on the continental slope above the wreck site shows little evidence of mass movements (Fig. 5). Isolated slide scars and turbidity-current channels have been mapped to the north (Fig. 3c, d), along with a possible presence of gullies on the upper slope below the shelf break inferred from IBSCO bathymetry (Fig. 2a). However, such features are no closer than about 200 km to the wreck site, and multibeam lines closer to the search area show a relatively smooth sea-floor typified by sedimentary lenses of acoustic Facies C (Fig. 4). Importantly, these lenses are capped by a crudely laminated drape of about 10 m in thickness (Fig. 5), indicating low-energy sedimentation over the past 10,000 years since regional deglaciation of the continental shelf east of the Antarctic Peninsula (e.g. Ó Cofaigh et al., 2014).

The sea-floor of the continental shelf east of the Peninsula has been heavily reworked by the ploughing action of iceberg keels down to modern water depths of 620 m (Fig. 3a, b). Ploughmarks deeper than the keels of icebergs calved from the modern Larsen C Ice Shelf (maximum 320 m) are likely to have been produced during regional deglaciation between about 14 and 10.5 kyr ago. The maximum observed depth of ploughmark occurrence on Antarctic continental shelves is typically 500-600 m (e.g. Barnes and Lien, 1988; Dowdeswell and Bamber, 2007), and ploughmarks at 700-800 m depth are exceptional (e.g. Gales et al., 2016; Wise et al., 2017). The *Endurance* wreck site is therefore at least 2,000 m below the keel-depths of even exceptionally thick icebergs and damage to the vessel's remains by this mechanism will not have taken place. The likely maximum keel-depths of even ridged multi-year sea in the Weddell Sea are no more than 20 m at most, and so this is also no threat to the integrity of the wreck. Thus, our marine-geophysical observations from the shelf-slope system in the western Weddell Sea, around and upslope of the wreck site,

suggest that the *Endurance* is likely to have been both undisturbed and unburied since it sank in 1915.

Arguably, the main difficulty in any attempt to discover and image the wreck using, for example, autonomous and remotely-operated vehicles (AUVs and ROVs), is therefore the severe sea-ice conditions in the western Weddell Sea. Without doubt, an icebreaking research vessel would be required any year for which we have observations of late-summer sea-ice conditions (Figs. 6, 7). Even in the most favourable year for which observations are available, 2002, sea-ice cover was between 40 and 90% around the wreck site and in every year since then the cover has been 90-100% (Fig. 6). Indeed, 90% and often 100% sea-ice cover often extends several hundred kilometres from the wreck site, making any approach slow at best. This level of sea-ice cover poses problems not just for icebreaker access, but also for the launch and recovery of AUVs and ROVs that might be used to investigate the wreck site in detail. Sea-ice hazard is probably the main reason why the wreck has remained undiscovered since the loss of *Endurance* almost a century ago. The Weddell Sea, and particularly the western side of the clockwise gyre, therefore remains one of the World's least accessible oceans because of these extreme sea-ice conditions (Figs. 6, 7).

Summary and conclusions

- We have used marine-geophysical evidence on sea-floor morphology and shallow acoustic stratigraphy to examine the nature of the substrate both around the relatively well-known location at which *Endurance* sank and for the part of the continental slope-shelf sedimentary system above this site on the western side of the Weddell Sea.

- Few signs of turbidity-current and mass-wasting activity are found either near or upslope of the wreck site, and any such activity was probably linked to full-glacial higher energy conditions when the Antarctic Peninsula Ice Sheet last advanced across the western Weddell Sea continental shelf about 20,000 years ago.

- The wreck site is well below the maximum depth of iceberg and sea-ice keels and *Endurance* will not have been damaged by ice-keel ploughing of the sea-floor.

- Thus, *Endurance* has remained undisturbed by submarine mass-wasting and has probably been draped by only a few centimetres of fine-grained sediment since it sank in 1915.

- Severe sea-ice conditions in the western Weddell Sea almost every year since 2002, a year of unusually low sea-ice cover when access was relatively easier, would hamper access to the wreck site.

- Accessing and investigating the wreck of Sir Ernest Shackleton's ship *Endurance* in the Weddell Sea therefore represents a significant challenge.

- An icebreaking research vessel is required in any year for which we have observations and even this would not guarantee that the site could be reached.

- High-resolution satellite imagery revealed the presence of open-water leads proximal to and extending within the wreck site in February 2019, enabling SA *Agulhas II* access to this sector of the Weddell Sea.

- Sea-ice cover approaching 100% at the wreck site during most austral summers may also pose difficulties for the launch and recovery of AUVs and ROVs deployed to investigate the *Endurance* wreck in detail.

- As the fate of Shackleton and his ship demonstrated a century ago, and our data show for the modern period, the sea ice of the Weddell Sea makes navigation and access problematic.

Author contributions

JAD wrote the initial manuscript, on which all authors provided comments. Geophysical data were collected by AWI authors and sea-ice data were contributed from SPRI. CLB drafted the figures.

References

Anderson, J.B., 1999. Antarctic Marine Geology, Cambridge University Press.

Anderson, J.B. and Andrews, J.T., 1999. Radiocarbon constraints on ice sheet advance and retreat in the Weddell Sea, Antarctica. Geology 27, 179-182.

Arndt, J.E., Schenke, H.W., Jakobsson, M., Nitschem, F., Buys, G., Goleby, B., Rebesco, M., Bohoyo, F., Hong, J., Black, J, Greku, R., Udintsev, G., Barrios, F., Reynoso-Peralta, W., Taisei, M., Wigley, R., 2013. The International Bathymetric Chart of the Southern Ocean (IBCSO) Version 1.0 – A new bathymetric compilation covering circum-Antarctic waters. Journal of Geophysical Research 40, 3111-3117.

Barnes, P.W., Lien, R., 1988. Icebergs rework shelf sediments to 500 m off Antarctica. Geology 16, 1130-1133

Bathmann, U., Smetacek, V., de Baar, H.J.W., Fahrbach, E., Krause, G., 1994. Die Expeditionen ANTARKTIS X/6-8 des Forschungsschiffes *Polarstern* 1992/93 (The Expeditions ANTARKTIS-X/6-8 of the Research Vessel *Polarstern* in 1992/93). Berichte zur Polarforschung - Reports on Polar Research, 135, 235 pp, https://doi.org/10.2312/BzP_0135_1994.

Bergman, L., Stuart, R.G., 2018. On the location of Shackleton's vessel *Endurance*. Journal of Navigation, doi:10.1017/S0373463318000619.

Beyer, A., Koltsova, A., Dieckmann, G., Haas, C., Schröder, M., 2007. Topography and structure of the upper layers of sediments of the ocean floor. ANT-XX11/2; 6 November 2004-19 January 2005; Cape Town-Cape Town; Ice Station *Polarstern* (ISPOL), 551, 204-209.

Cavalieri, D. J., Parkinson, C.L., Gloersen, P., Zwally, H.J., 1996, updated yearly. Sea Ice Concentrations from Nimbus-7 SMMR and DMSP SSM/I-SSMIS Passive Microwave Data, Version 1. (Weddell Sea subset). Boulder, Colorado USA. NASA National Snow and Ice Data Center Distributed Active Archive Center. doi: https://doi.org/10.5067/8GQ8LZQVL0VL. Accessed September 2019

Campo, J.M., Wellner, J.S., Domack, E., Lavoie, C., Yoo, K-C., 2017. Glacial geomorphology of the northwestern Weddell Sea, eastern Antarctic Peninsula continental shelf: Shifting ice flow patterns during deglaciation. Geomorphology 280, 89-107.

Comiso, J. C., Parkinson, C. L., Gersten, R., Stock, L., 2008. Accelerated decline in the Arctic sea ice cover, Geophysical Research Letters 35, doi:10.1029/2007GL031972

Damuth, J.E., 1978. Echo-character of the Norwegian-Greenland Sea: relationship to Quaternary sedimentation. Marine Geology 28, 1-36.

Deacon, G.E.R., 1979. The Weddell Gyre. Deep-Sea Research 26, 981-995.

Dijkstra, S. J., Stober, M., Tsoukalas, N., Schenke, H.W., 2011. Swath sonar bathymetry during *Polarstern* cruise ANT-XIV/3 (PS43) with links to multibeam raw data files. Alfred

Wegener Institute, Helmholtz Centre for Polar and Marine Research, Bremerhaven, PANGAEA, https://doi.org/10.1594/PANGAEA.763232.

Dowdeswell, J.A., Bamber, J.L., 2007. Keel depths of modern Antarctic icebergs and implications for sea-floor scouring in the geological record. Marine Geology 243, 120-131.

Dowdeswell, J.A., Ó Cofaigh, C., Noormets, R., Larter, R.D., Hillenbrand, C.-D., Benetti, S., Evans, J., Pudsey, C.J., 2008. A major trough-mouth fan on the continental margin of the Bellingshausen Sea, West Antarctica: The Belgica Fan. Marine Geology 252, 129-140.

Dowdeswell, J.A., Evans, J., Ó Cofaigh, C., 2010. Submarine landforms and shallow acoustic stratigraphy of a 400 km-long fjord-shelf-slope transect, Kangerlussuaq margin, East Greenland. Quaternary Science Reviews 29, 3359-3369.

El Naggar, S. El D., Dieckmann, G. S., Haas, C., Schröder, M., Spindler, M., 2007. The Expeditions ANTARKTIS-XXII/1 and XXII/2 of the Research Vessel *Polarstern* in 2004/2005. Berichte zur Polar- und Meeresforschung - Reports on Polar and Marine Research, 551, 259 pp, https://doi.org/10.2312/BzPM_0551_2007.

Evans, J., Pudsey, C.J., Ó Cofaigh, C., Morris, P., Domack, E., 2005. Late Quaternary glacial history, flow dynamics and sedimentation along the eastern margin of the Antarctic Peninsula Ice Sheet. Quaternary Science Reviews 24, 741-774.

Fillinger, L., Gutt, J., Schenke, H.W., 2011. Swath sonar bathymetry during *Polarstern* cruise ANT-XXVII/3 (PS77, CAMBIO) with links to multibeam raw data files. Alfred Wegener Institute, Helmholtz Centre for Polar and Marine Research, Bremerhaven, PANGAEA, https://doi.org/10.1594/PANGAEA.766940.

Frantz, C.M., Light, B., Farley, S. M., Carpenter, S., Lieblappen, R., Courville, Z., Orellana, M.V., Junge, K., 2019. Physical and optical characteristics of heavily melted "rotten" Arctic sea ice. The Cryosphere 13, 775-793, doi:10.5194/tc-13-775-2019.

Gales, J.A., Larter, R.D., Leat P.T., 2016. Iceberg ploughmarks and associated sediment ridges on the southern Weddell Sea margin. In Dowdeswell, J.A. et al., (eds), Atlas of Submarine Glacial Landforms: Modern, Quaternary and Ancient. Geological Society, London, Memoirs 46, 289-290.

Gutt, J., 2008. The Expedition ANTARKTIS-XXIII/8 of the Research Vessel *Polarstern* in 2006/2007. Berichte zur Polar- und Meeresforschung - Reports on Polar and Marine Research, 569, 153 pp, https://doi.org/10.2312/BzPM_0569_2008.

Gutt, J., Barratt, I., Domack, E. W., d'Udekem d'Acoz, C., Dimmler, W., Grémare, A., Heilmayer, O., Isla, E., Janussen, D., Jorgensen, E., Kock, K-H., Lehnert, L. S., López-Gonzáles, P. J., Langner, S., Linse, K., Manjón-Cabeza, M. E., Meißner, M., Montiel, A. R., Maarten; R. H., Rose, A., Schepisi, E. S., Saucède, T., Scheidat, M., Schenke, H. W., Seiler, J., Smith, C. 2010. Swath sonar bathymetry during *Polarstern* cruise ANT-XXIII/8 (PS69) with links to multibeam raw data files. Alfred Wegener Institute, Helmholtz Centre for Polar and Marine Research, Bremerhaven, PANGAEA, https://doi.org/10.1594/PANGAEA.668088.

Hillenbrand, C.-D., Baesler, A., Grobe, H., 2005. The sedimentary record of the last glaciation in the western Bellingshausen Sea (West Antarctica): Implications for the interpretation of diamictons in a polar-marine setting. Marine Geology 216, 191-204.

Howat, I.M., Porter, C., Smith, B.E., Noh, M.-J., Morin, P., 2019. The Reference Elevation Model of Antarctica. The Cryosphere 13, 665-674.

Jakobsson, M., Gyllencreutz, R., Mayer, L.A., Dowdeswell, J.A., Canals, M., Todd, B.J., Dowdeswell, E.K., Hogan K.A., Larter, R.D., 2016. Mapping submarine glacial landforms using acoustic methods. In Dowdeswell, J.A. et al., (eds), Atlas of Submarine Glacial Landforms: Modern, Quaternary and Ancient. Geological Society, London, Memoirs 46, 17-40.

Jokat, W., Krause, G., 2003. Die Expedition ANTARKTIS XIX mit FS *Polarstern* 2001/2002 Bericht von den Fahrtabschnitten 1 und 2 (The Expedition ANTARKTIS XIX of RV Polarstern in 2001/2002 reports of legs 1 and 2). Berichte zur Polar- und Meeresforschung = Reports on Polar and Marine Research, 448, 78 pp, https://doi.org/10.2312/BzPM_0448_2003

Jokat, W., Oerter, H., 1998. Die Expedition ANTARKTIS-XIV mit FS *Polarstern* 1997, Bericht vom Fahrtabschnitt ANT-XIV/3 (The Expedition ANTARKTIS-XIV of RV *Polarstern* in 1997 Report of Leg ANT-XIV/3). Berichte zur Polarforschung = Reports on Polar Research, 267, 236 pp, https://doi.org/10.2312/BzP_0267_1998.

Kern, S., Ozsoy-Çiçek, B., Worby, A.P., 2016. Antarctic sea-ice thickness retrieval from ICESat: Intercomparison of different approaches. Remote Sensing 8, 538; doi:10.3390/rs8070538.

King, E.L., Haflidason, H., Sejrup, H.P., Løvlie, R., 1998. Glacigenic debris flows on the North Sea Trough Mouth Fan during ice stream maxima. Marine Geology 152, 217–246.

Kurtz, N.T., Markus, T., 2012. Satellite observations of Antarctic sea ice thickness and volume. Journal of Geophysical Research, 117, doi:10.1029/2012JC008141.

Lelouche. J-M., Legalloudec, O., Regnier, C., Levier, B., Greiner, E., Drevillon, M. 2019. Quality Information Document for Global Sea Physical Analysis and Forecasting Product GLOBAL_ANALYSIS_FORECAST_PHY_001_024, Issue 2.1, 30/04/2019. Obtained online (Nov 2019) at: marine.copernicus.eu/documents/QUID/CMEMS-GLO-QUID-001-024.pdf

Miles, B.W.J., Stokes, C.R., Jamieson, S.S.R., 2017. Simultaneous disintegration of outlet glaciers in Porpoise Bay (Wilkes Land), East Antarctica, driven by sea ice break-up. The Cryosphere 11, 427-442.

Muench, R.L. and Gordon, A.L., 1995. Circulation and transport of water along the western Weddell Sea margin. Journal of Geophysical Research 100, 18503-18515.

Ó Cofaigh, C., and 17 others, 2014. Reconstruction of ice-sheet changes in the Antarctic Peninsula since the Last Glacial Maximum. Quaternary Science Reviews 100, 87-110.

Picard, K., Brooke, B.P., Harris, P.T., Siwabessy, P.J.W., Coffin, M.F., Tran, M., Spinoccia, M., Weales, J., Macmillan-Lawler, M., Sullivan, J., 2018. Malaysia Airlines flight MH370 search data reveal geomorphology and seafloor processes in the remote southeast Indian Ocean. Marine Geology 395, 301-319.

Pudsey, C.J., Murray, J.W., Appleby, P., Evans, J., 2006. Ice shelf history from petrographic and foraminiferal evidence, northeast Antarctic Peninsula. Quaternary Science Reviews 25, 2357-2379.

Ryan, S., Schröder, M., Huhn, O., Timmermann, R., 2016. On the warm inflow at the eastern boundary of the Weddell Gyre. Deep-Sea Research Part I: Oceanographic Research Papers 107, 70-81.

Schenke, H.W., 2011. Swath sonar bathymetry during *Polarstern* cruise ANT-X/7 (PS23) with links to multibeam raw data files. Alfred Wegener Institute, Helmholtz Centre for Polar and Marine Research, Bremerhaven, PANGAEA, https://doi.org/10.1594/PANGAEA.763386.

Schenke, H. W., Beyer, A., Koltsova, A., 2009. Swath sonar bathymetry during *Polarstern* cruise ANT-XXII/2 (PS67) with links to multibeam raw data files. Alfred Wegener Institute, Helmholtz Centre for Polar and Marine Research, Bremerhaven, PANGAEA, https://doi.org/10.1594/PANGAEA.724659.

Schenke, H. W., Büchsenschütz-Nothdurft, O., Krocker, R., Lindner, K., Iffland, A., 2004. Swath sonar bathymetry during *Polarstern* cruise ANT-XIX/2 (PS61) with links to multibeam raw data files. Alfred Wegener Institute, Helmholtz Centre for Polar and Marine Research, Bremerhaven, PANGAEA, https://doi.org/10.1594/PANGAEA.701695.

Shackleton, E.A., 1919. South: The Story of Shackleton's Last Expedition 1914-17. Heinemann, London, 376 pp.

Tan, B., Li, Z-j., Lu, P., Haas, C., Nicolaus, M., 2012. Morphology of sea ice pressure ridges in the northwestern Weddell Sea in winter. Journal of Geophysical Research 117, doi:10.1029/2011JC007800.

Thoma, M., Grosfeld, K., Mohrholz, C-O., Lange, M.A., 2005. Modelling ocean circulation and ice-ocean interaction in the southeastern Weddell Sea. Forum for Research into Ice Shelf Processes (FRISP) Report 16.

Vernet, M., Geibert, W., Hoppema, M., Brown, P. J., Haas, C., Hellmer, H. H., et al. (2019). The Weddell Gyre, Southern Ocean: Present knowledge and future challenges. Reviews of Geophysics, 57. https://doi.org/10.1029/ 2018RG0 00604

Wise, M.G., Dowdeswell, J.A., Jakobsson, M., Larter, R.D., 2017. Evidence of marine ice-cliff instability in Pine Island Bay from iceberg-keel ploughmarks. Nature 550, 506-510.

Worby, A.P., Geiger, C.A., Paget, M.J., Van Woert, M.L., Ackley, S.F., DeLiberty, T.L., 2008. Thickness distribution of Antarctic sea ice. Journal of Geophysical Research 113, doi:10.1029/2007JC004254.

Wordie, J.M., 1921. Shackleton Antarctic Expedition. 1914-1917: Depths and Deposits of the Weddell Sea. Transactions of the Royal Society of Edinburgh 52, Pt. iii, No. 30.

Worsley, F.A. 1931. Endurance: an Epic of Polar Adventure. Allan, London, 316 pp.

Zwally, H. & Gloersen, P., 1977. Passive microwave images of the polar regions and research applications. Polar Record 18, 431-450.

Figure Captions

Figure 1. (a) Map showing the route taken by *Endurance*/'Ocean Camp' and *James Caird* lifeboat, as compiled by Reginald James using Frank Worsley's navigation measurements. Water depths are from ETOPO1 1 arc-minute global relief of the Earth's surface (http://www.ngdc.noaa.gov/mgg/global/). Contours are every 500 m. Height of the Antarctic Ice Sheet is from the Reference Elevation Model of Antarctica (REMA) Digital Elevation Model (DEM) (Howat *et al.*, 2019). B = Brunt Ice Shelf; E = Ekström Ice Shelf; J = Jelbart Ice Shelf; RL = Riiser-Larsen Ice Shelf; SW = Stancomb-Wills Ice Shelf. (b) Photograph showing *Endurance* beset in sea ice just before her sinking (© Scott Polar Research Institute). (c) Photograph showing *James Caird* setting out from Elephant Island towards South Georgia on 24 April 1916 (© Scott Polar Research Institute).

Figure 2. (a) Bathymetric map of the western Weddell Sea showing data collected by the Alfred Wegener Institute (AWI) on board the RV *Polarstern.* Pink box shows the search area for the wreck of the *Endurance* defined for the Weddell Sea Expedition 2019*,* which spans 20 nautical miles around the location of Ocean Camp. The distribution of sea-floor disturbances (iceberg ploughmarks, slide scarps and slope channels), mapped from the AWI dataset, is shown. Background shows the International Bathymetric Chart of the Southern Ocean (IBCSO) bathymetry (Arndt *et al.*, 2013) at 500 m resolution with 200 m contours (dark grey), and 100 m contours (light grey) in regions of the sea-floor shallower than 1,000 m. Grey shading denotes terrestrially grounded ice; white, the spatial extent of the western Weddell Sea's ice shelves. The location of iceberg A-68 prior to its calving from Larsen C Ice Shelf is also shown (blue shading), in addition to its observed location in September 2018 (translucent white shading). (b) Detail of the sea-floor close to the location of Ocean Camp (2,970 m water depth). Grid-cell size 100 m.

Fig. 3. Examples of sea-floor disturbances on the shelf and slope of the western Weddell Sea. (a) Frequency distribution of the depth of iceberg ploughmarks in the study area. The deepest draft of modern icebergs is from Dowdeswell and Bamber (2007). (b) Detail of iceberg ploughmark in around 470 m water depth. (c) Profile across the iceberg ploughmarks at about 470 m water depth. (c) and (d) Details of a slide scar and channel on the continental slope. Locations are shown in Fig. 2a.

Fig. 4. Acoustic facies in the western Weddell Sea, derived from AWI PARASOUND sub-bottom profiler data. (a) Map showing the distribution of the five main acoustic facies. Pink box shows the Weddell Sea Expedition 2019 search area for the wreck of *Endurance*, which spans 20 nautical miles around the location of Ocean Camp (pink circle). (b) to (e) Examples of Facies A to D, respectively. TWT = two-way travel time.

Fig. 5. (a) Long-profile of the continental slope close to the location of the *Endurance* wreck site, derived from AWI sub-bottom profiler PARASOUND and bathymetric data. Profile is located in Fig. 3a. (b) and (c) Details of the acoustic character of the lower slope. Data gaps are often produced by sea ice interference with the sonar system.

Fig. 6. (a) Satellite image composite formed from Moderate Resolution Imaging Spectroradiometer (MODIS) and Visible Infrared Imaging Radiometer Suite (VIIRS) imagery acquired between 29 January and 4 February 2019 (resolution *c.* 250 m). Yellow shading denotes persistent cloud cover. Red box shows the search area for the wreck of the *Endurance*, following Figure 2a. Dashed line is iceberg A-68. LC = Larsen C Ice Shelf. (b) to (d) Sea-ice average concentration summary images for February for the western Weddell Sea, showing three typical scenarios for accessing the search area for the wreck of the *Endurance* (white box): (b) 'Good' (2002), (c) 'Intermediate' (2019; the route of the SA *Agulhas II* during the Weddell Sea Expedition 2019 is shown in white), and (d) 'Bad' (2014). Key in (c) and (d) is the same as (b). (e) Plot showing the changing average December-January-February sea-ice conditions in the western Weddell Sea between 2002 and 2019 (inclusive), as assessed using qualitative rankings.

Fig. 7. (a) Same as Fig. 6c, zoomed over the central Weddell Sea. TerraSAR-X Stripmap and ScanSAR imagery used for navigation purposes on the approach to the Endurance wreck search area (red box) are shown superimposed on part of the MODIS/VIIRS composite image

in Figure 6c. The route of the SA *Agulhas II* during the Weddell Sea Expedition 2019 is shown in white. (b) TerraSAR-X full resolution Spotlight image showing the presence of large leads in the search area, with ship track in white. (c) Detail showing typical sea-ice conditions encountered by the SA *Agulhas II* during the search for *Endurance*, with ship track in white (TerraSAR-X data © Deutsches Zentrum für Luft-und Raumfahrt/DLR).
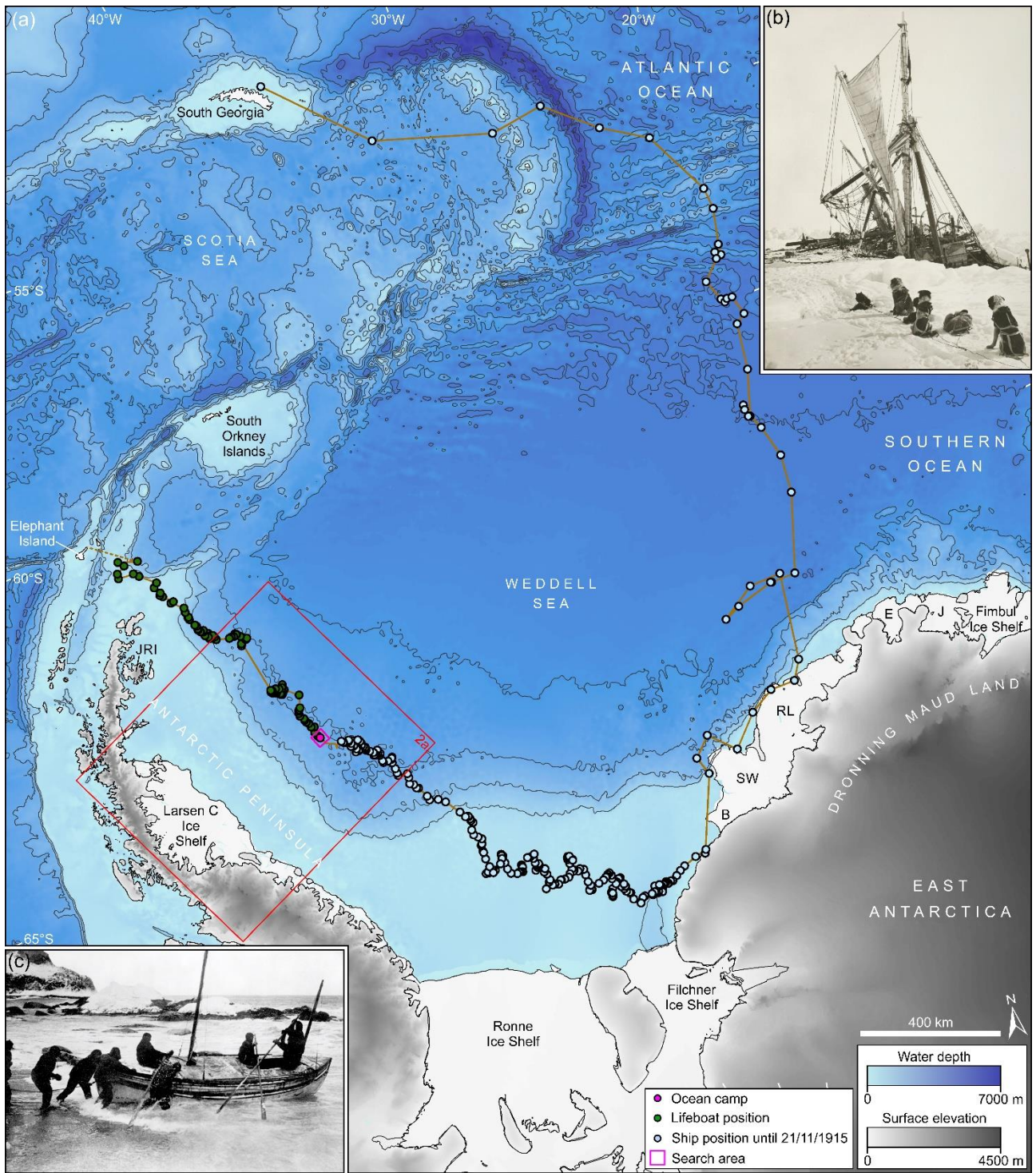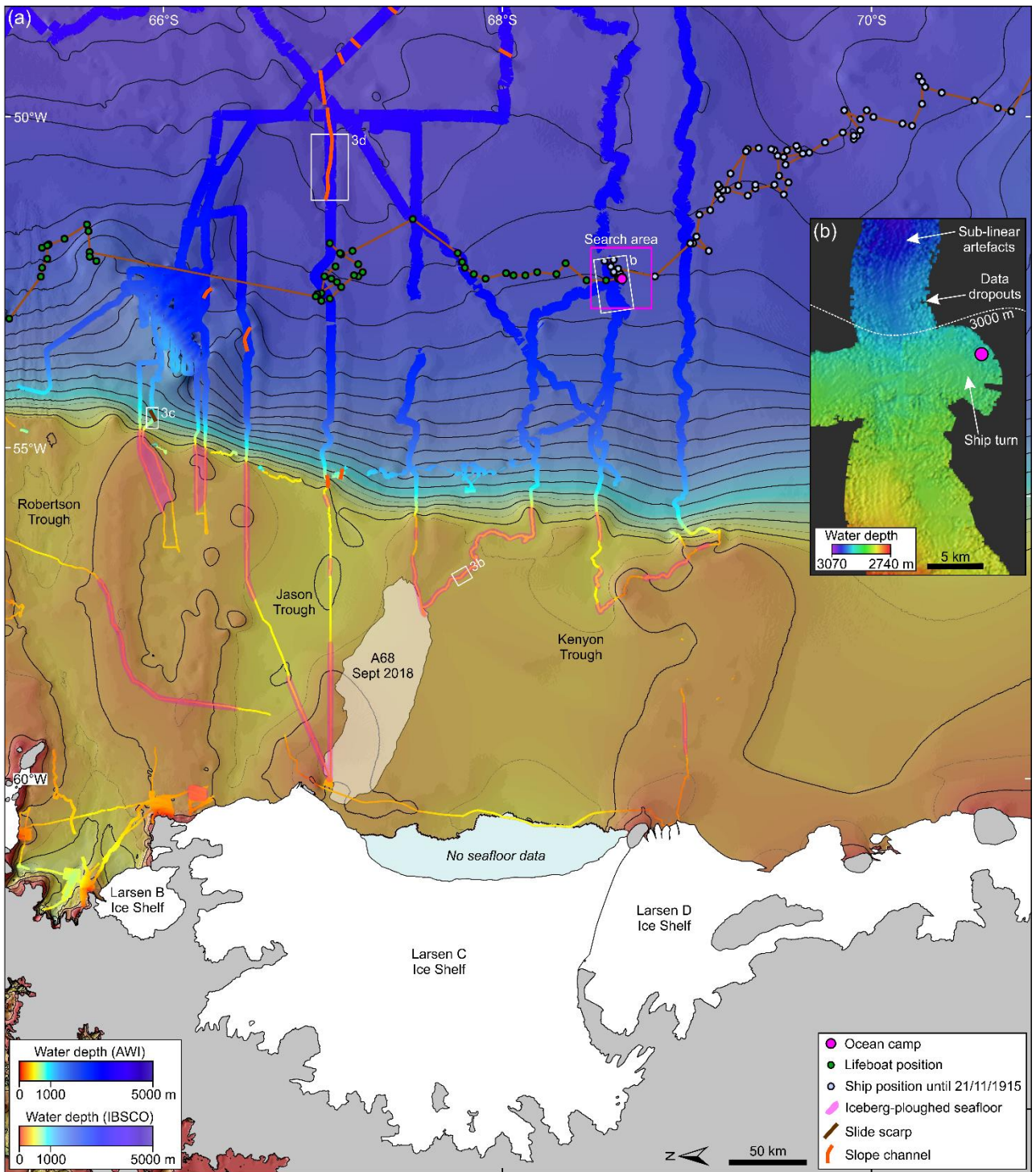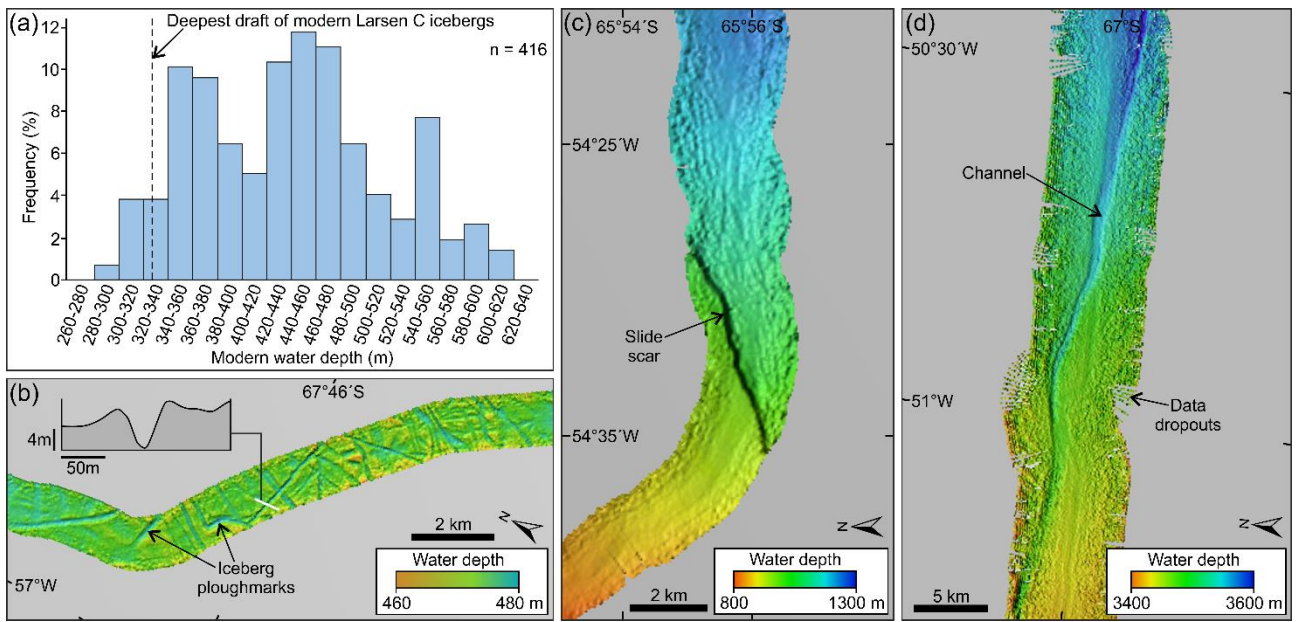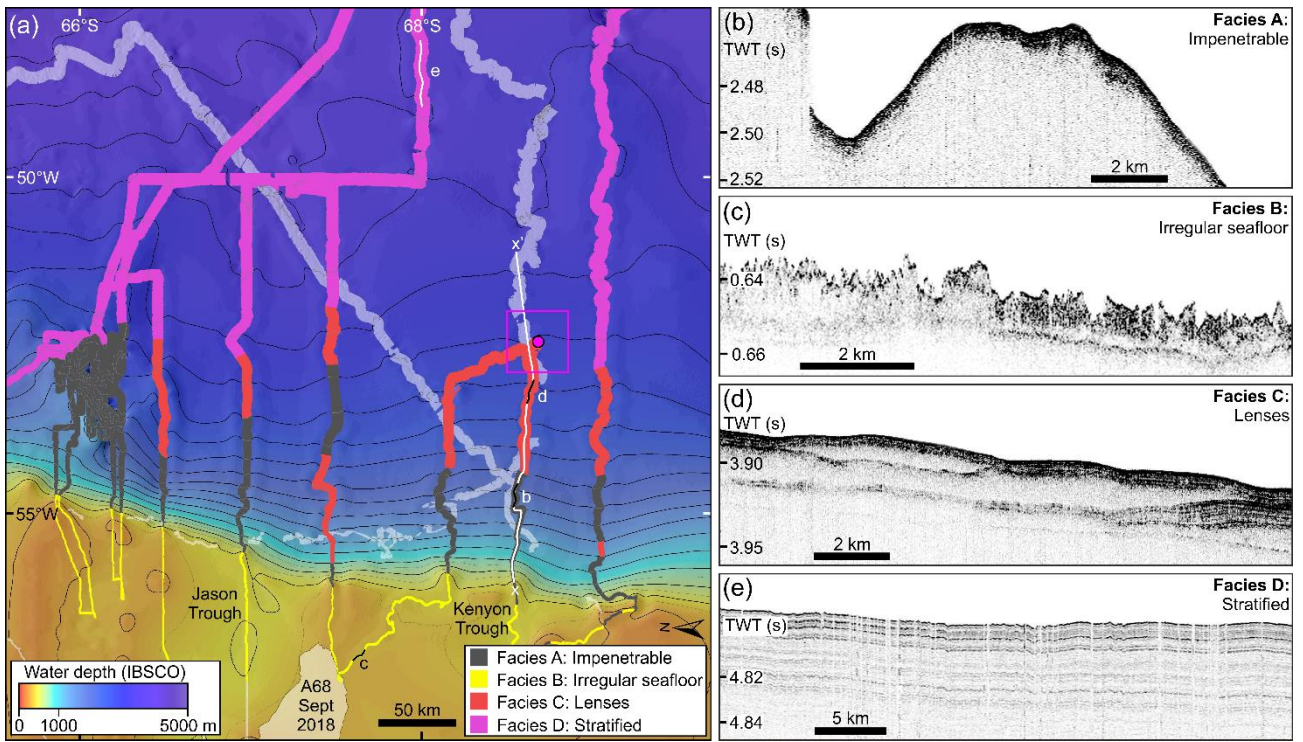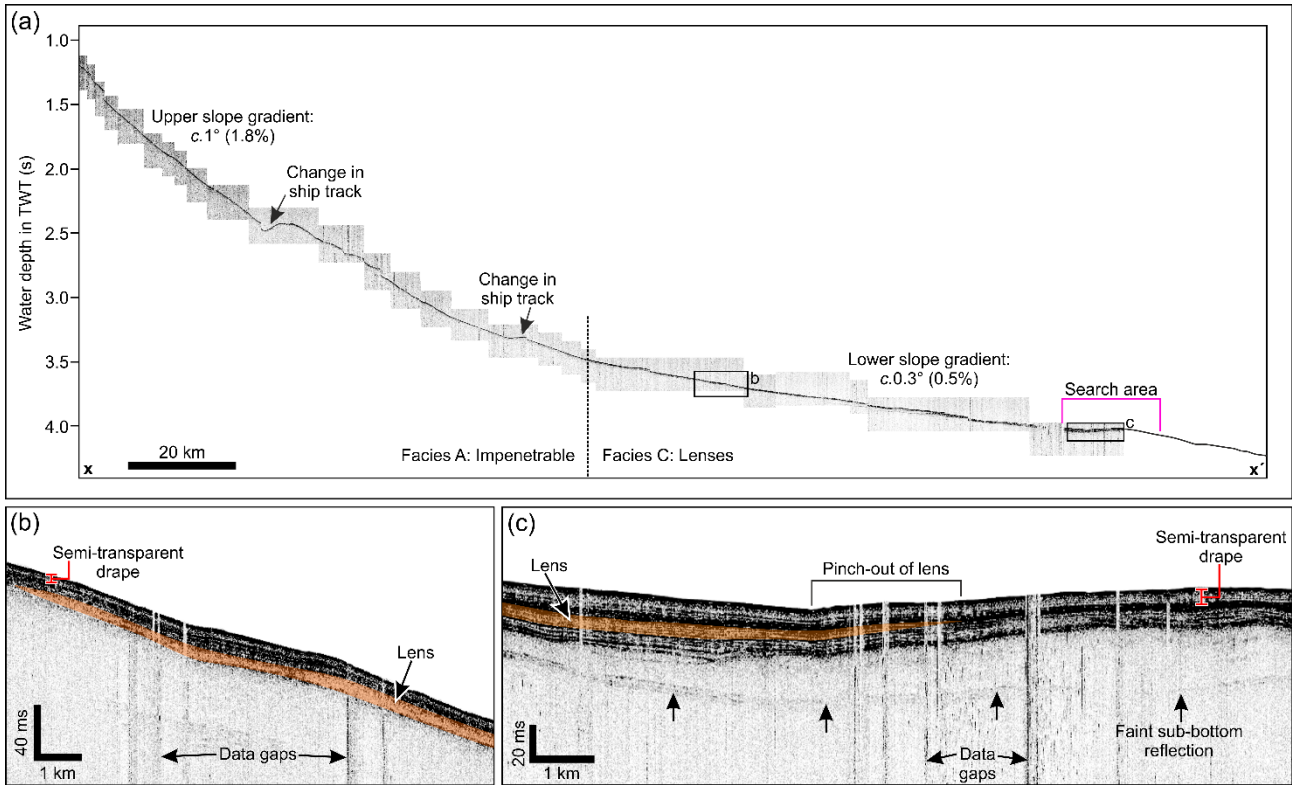
Figure 1

Figure 2

Figure 3

Figure 4

Figure 5

Figure 6

Figure 7